Available online at www.sciencedirect.com

ScienceDirect

Journal of Computational and Applied Mathematics 198 (2007) 1 – 18

JOURNAL OF COMPUTATIONAL AND APPLIED MATHEMATICS

www.elsevier.com/locate/cam

Eigenfrequencies of fractal drums

Lehel Banjai*

Max-Planck-Institut für Mathematik in den Naturwissenschaften, Inselstraße 22–26, D-04103 Leipzig, Germany

Received 8 March 2005; received in revised form 24 October 2005

Abstract

A method for the computation of eigenfrequencies and eigenmodes of fractal drums is presented. The approach involves first conformally mapping the unit disk to a polygon approximating the fractal and then solving a weighted eigenvalue problem on the unit disk by a spectral collocation method. The numerical computation of the complicated conformal mapping was made feasible by the use of the fast multipole method as described in [L. Banjai, L.N. Trefethen, A multipole method for Schwarz–Christoffel mapping of polygons with thousands of sides, SIAM J. Sci. Comput. 25(3) (2003) 1042–1065]. The linear system arising from the spectral discretization is large and dense. To circumvent this problem we devise a fast method for the inversion of such a system. Consequently, the eigenvalue problem is solved iteratively. We obtain eight digits for the first eigenvalue of the Koch snowflake and at least five digits for eigenvalues up to the 20th. Numerical results for two more fractals are shown.

MSC: 65N25; 65N35; 35P99; 30C20

Keywords: Fractals; Eigenvalues; Spectral methods; Conformal transplantation

1. Introduction

Objects in nature are not always well represented by simple geometries such as circles or straight lines. As evidence for this Mandelbrot [24,25] used the experiments by Richardson to show that some coastlines are better modelled by curves of infinite length than by compositions of smooth curves. The overwhelming evidence that objects in nature can be modelled by fractals leads to the question of how physical processes on fractals can be described. Also some physical processes seem to generate fractals [37].

One particular physical process that has attracted theoretical [19,21], experimental [31], and numerical investigation [15,20] is the mechanical vibration of a fractal drum. The hope is that research in this direction might shed light on such problems as the dependence of sea waves on topography of the coastline. The mere existence of fractal coastlines suggests good damping properties of fractal shapes [30].

In this paper, we develop a numerical method for the computation of the eigenvalues and eigenfunctions of the Dirichlet Laplacian on fractal domains. We approximate a fractal with a polygon of many thousands of vertices and solve the eigenvalue problem on this polygon. Numerical solution of eigenvalue problems on polygons is a classical problem, see [13], and has recently been very successfully solved for polygons with few vertices [3,7]. However, all of

* Tel.: +41 0 44 63 55856; fax: +41 0 44 63 55705.
E-mail address: banjai@mis.mpg.de.

0377-0427/$ - see front matter © 2005 Elsevier B.V. All rights reserved.
doi:10.1016/j.cam.2005.11.015

these methods become too expensive once the number of vertices of the polygon runs into thousands. Hence alternative methods are required when the domain of interest is a fractal.

As our main example we study the steady-state vibrations of a Koch snowflake drum. Computations of eigenvalues and eigenfunctions of such a system have already been done by using finite differences on polygonal approximations to the fractal domain [20]. Using their numerical results Lapidus et al. have produced beautiful images of eigenmodes; these images have subsequently been realized as mathematical sculptures by the artist Helaman Ferguson [10]. Recently, a different grid for the finite differences has been used to obtain more accurate results [27].

Our method consists of transplantation from a Koch snowflake polygon to the unit disk and then the solution of the modified eigenvalue problem on the unit disk by a spectral collocation method. The idea of using conformal mapping to simplify the computational domain is by no means new. The more common approach to solving Poisson equations is to map the domain onto a rectangle and then use finite difference or finite element discretizations on the rectangle; for a review of this and many other applications of conformal mapping see [32]. Cureton and Kuttler [5] have computed eigenvalues of the hexagon by conformally mapping the domain to the unit disk and then applying the Rayleigh–Ritz method, with the eigenfunctions of the unweighted problem on the disk as the trial functions. Mason uses a conformal map to straighten the reentrant corner of the L-shaped membrane and then applies a spectral method to the transplanted problem [26].

In numerical experiments we find that, whereas previous studies have achieved around three [20] or four [27] digits of accuracy, this method appears to provide at least five and up to eight digits, depending on the eigenvalue, not only for the approximating polygons but also for the Koch snowflake fractal. We do not prove that our results are this accurate, but the experimental evidence is compelling. We also compute eigenvalues for further two fractals. One is an example of a fractal for which our method works even better than for the Koch snowflake whereas for the second it performs less well. We give reasons why such a behaviour is to be expected.

2. Statement of the problem

Let $\Omega \subset \mathbb{R}^2$ be a bounded simply-connected domain. We consider the situation where a homogeneous membrane is stretched and then fixed along its boundary $\partial\Omega$ and the tension per unit length caused by stretching is the same at all points and all directions and does not change during motion. Let $U(x, y, t)$ be a function that gives the displacement of the membrane at point $(x, y) \in \mathbb{R}^2$ and at time $t \geqslant 0$. Then U satisfies the wave equation

$$U_{tt} = \Delta U, \tag{1}$$

with boundary condition

$$U(x_0, y_0, t) = 0, \quad (x_0, y_0) \in \partial\Omega. \tag{2}$$

By separation of variables $U(x, y, t) = u(x, y)w(t)$ the wave equation gives

$$w''(t) + \lambda w(t) = 0,$$

$$\Delta u + \lambda u = 0 \quad \text{in } \Omega,$$

where $\lambda > 0$ is a constant. Since the first equation is trivial we concentrate on finding the eigenvalue-eigenfunction pairs (λ, u) such that

$$\begin{aligned} &\Delta u + \lambda u = 0 \quad \text{in } \Omega, \\ &u = 0 \quad \text{on } \partial\Omega. \end{aligned} \tag{3}$$

It is known that the spectrum of the Dirichlet Laplacian is discrete and consists of an infinite sequence of eigenvalues $\{\lambda_i\}$

$$0 < \lambda_1 < \lambda_2 \leqslant \cdots \leqslant \lambda_n \leqslant \cdots$$

such that $\lambda_n \to \infty$ as $n \to \infty$; see [6]. The corresponding eigenfunctions u_n are infinitely differentiable in Ω and u_1 can be chosen so that $u_1 > 0$.

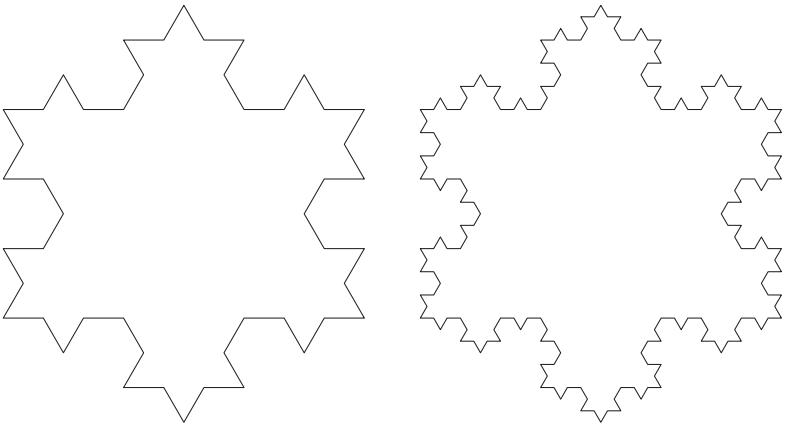

Fig. 1. Polygon P_3 is shown on the left and polygon P_4 on the right.

Naturally we can only expect to be able to solve the problem on an approximation to the fractal domain. Let us denote the fractal domain by Φ. We choose to approximate Φ by a sequence of polygons P_n, see Fig. 1 for the case of the Koch snowflake, and solve the eigenvalue problem on these polygons. The sequence is such that $P_n \subset P_{n+1}$ and $P_n \to \Phi$ as $n \to \infty$. The following result, which can be found in Davies [6], confirms the existence of a discrete spectrum on the fractal and justifies our intuition that as the polygons become better approximations to the fractal the eigenvalues also converge to the eigenvalues on the fractal.

Theorem 1. *Let Ω be a bounded region in $\mathbb{R}^N$, and let $\mathscr{L}$ be the negative of the Dirichlet Laplacian acting on $L^2(\Omega)$. Then $\mathscr{L}$ has empty essential spectrum and compact resolvent. The nth eigenvalue $\lambda_n(\Omega)$ of $\mathscr{L}$ is a monotonically decreasing function of the region, and if Ω_m is an increasing sequence of regions with union equal to Ω then*

$$\lim_{m\to\infty} \lambda_n(\Omega_m) = \lambda_n(\Omega)$$

for all $n \geqslant 1$.

3. Conformal transplantation

As mentioned in the introduction, before we attempt to solve the eigenvalue problem we shall transplant the problem to a simpler domain. The following result gives the necessary theory for the method of conformal transplantation; see also Fig. 2. Note that for convenience we identify the set of ordered pairs $\mathbb{R}^2$ with the complex plane $\mathbb{C}$ in the usual way and use the two representations interchangeably.

Theorem 2. *If (λ, u) is a solution of the eigenvalue problem* (3) *and if f is a holomorphic function defining a one-to-one mapping of a region D onto the region Ω, then $u = v \circ f^{-1}$, where (λ, v) is a solution of the eigenvalue problem*

$$\begin{aligned} &\Delta v + \lambda v |f'|^2 = 0 \quad \text{in } D, \\ &v = 0 \quad \text{on } \partial D. \end{aligned} \tag{4}$$

Proof. The result follows from the identity

$$\Delta_z u(z) = \Delta_w v(w) |f'(w)|^{-2}, \quad z \in \Omega,$$

where $w = f^{-1}(z)$. □

Using this result we can consider a weighted eigenvalue problem on a much simpler domain. Throughout this paper D is the unit disk and, since numerically we cannot deal with the fractal, Ω is a polygon P_n, for some $n > 1$, and hence

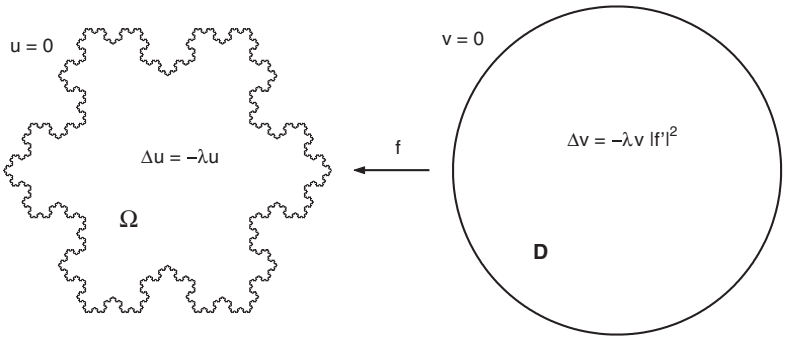

Fig. 2. Conformal transplantation of the eigenvalue problem.

f is a Schwarz–Christoffel map; see Fig. 2. To solve the transplanted problem we need to be able to evaluate f', which in the case we consider has the form

$$f'(w) = C \prod_{k=1}^{N} (w - w_k)^{\beta_k}, \tag{5}$$

where w_k are the preimages of the corners z_k of the polygon, i.e. $w_k = f^{-1}(z_k)$. The parameters, w_k and C, are not known initially and have to be computed. Once the parameters are determined, the above product can be evaluated extremely efficiently. A method for both computing the parameters and for rapid evaluation of such products that is applicable even for polygons with hundreds of thousands of vertices is described in [2]. Let us just state that the cost of finding all the parameters is $O(N \log N)$ and the cost of subsequent evaluation of the derivative at a single point inside the disk is $O(\log N)$. In the next section the regularity of the eigenfunctions of the original and of the transplanted problem are discussed.

4. Smoothness of eigenfunctions

Let (λ, u) be a solution of the original eigenvalue problem (3) where the domain Ω is not the fractal Φ but a certain polygonal approximation to it P_n. Then (λ, v) is a solution of the transplanted problem (4) with $v(w) = u \circ f(w)$, where f is the conformal map of the unit disk D onto $\Omega = P_n$. It is well known that $u \in C^\infty(\Omega)$; see [18]. Since f is an analytic function inside D we also have that $v \in C^\infty(D)$. Also the eigenfunction u can be reflected as a C^∞ function at any part of the boundary $\partial\Omega$ that is C^∞. Hence u can only be singular at the corners of the domain Ω and v can only be singular at the images of the corners under the map f^{-1}.

Let us choose a corner $z_0 \in \partial\Omega$ with interior angle π/α and let (r, ϕ) be the polar coordinates originating from that corner. Then

$$u(r, \phi) = \sum_{n=1}^{\infty} a_n J_{\alpha n}(\sqrt{\lambda}) \sin(\alpha n \phi), \tag{6}$$

where J_ν is a Bessel function of the first kind. Expanding the Bessel functions we get that

$$u(r, \phi) = a_0 r^\alpha \sin(\alpha\phi) + O(r^{2\alpha}) + O(r^{\alpha+2}). \tag{7}$$

If α is a positive integer the solution can be extended to a C^∞ function in the vicinity of such a corner; this can be seen either by reflection or by the above expansion. When α is not an integer the leading singularity is of the order r^α. In the case of the Koch snowflake this means that at an acute angle of the boundary, $\alpha = 3$, an eigenfunction has a removable singularity whereas at an obtuse angle, $\alpha = \frac{3}{4}$, the singularity has the leading order $r^{3/4}$.

The conformal map f is also singular at the preimages of the corners. If $z_k \in \partial\Omega$, $k = 0, \ldots, n$, are the corners with interior angles π/α_k, with $\alpha_0 = \alpha$, then f can be written as

$$f(w) = z_0 + C \int_{w_0}^{w} \prod_{k=0}^{n} (\zeta - w_k)^{1/\alpha_k - 1} \, \mathrm{d}\zeta,$$

where $w_k = f^{-1}(z_k)$ are the *prevertices* and C is some constant; see [8]. We are interested in the behaviour near the prevertex w_0 at some point $w = w_0 + \rho e^{i\theta} \in D$. In the following we will use the fact that $\prod_{k=1}^{n} (\zeta - w_k)^{1/\alpha_k - 1}$ is analytic and hence has a valid Taylor series in a neighbourhood of w_0.

$$\begin{aligned} f(w_0 + \rho e^{i\theta}) = f(w) &= z_0 + C \int_{w_0}^{w} (\zeta - w_0)^{1/\alpha - 1} \prod_{k=1}^{n} (\zeta - w_k)^{1/\alpha_k - 1} \, \mathrm{d}\zeta, \\ &= z_0 + C \int_{w_0}^{w} (\zeta - w_0)^{1/\alpha - 1} \sum_{m=0}^{\infty} b_m (\zeta - w_0)^m \, \mathrm{d}\zeta \\ &= z_0 + C \sum_{m=0}^{\infty} b_m \int_{w_0}^{w} (\zeta - w_0)^{m + 1/\alpha - 1} \, \mathrm{d}\zeta \\ &= z_0 + \sum_{m=0}^{\infty} c_m \rho^{m+1/\alpha} e^{i(m+1/\alpha)\theta}, \end{aligned}$$

for some constant coefficients $(b_m)_{m \geqslant 0}$ and $(c_m)_{m \geqslant 0}$. The interchange of integration and summation can be justified using integration by parts and the uniform convergence of the Taylor series. From above we conclude that near w_0

$$f(w_0 + \rho e^{i\theta}) = c_0 \rho^{1/\alpha} e^{i\theta/\alpha} + \mathrm{O}(\rho^{1+1/\alpha}). \tag{8}$$

Combining (7) and (8) we obtain, where (ρ, θ) are the polar coordinates originating at w_0, that

$$v(\rho, \theta) = d_0 \rho \sin(\theta) + \mathrm{O}(\rho^{1+\alpha}) + \mathrm{O}(\rho^{1+2/\alpha}). \tag{9}$$

This means that in the case of the Koch snowflake polygons, the singularity at the preimage of an obtuse corner is now of the leading order $\rho^{7/4}$ and at the preimage of an acute corner of the order $\rho^{5/3}$. Therefore, even though singularities have been introduced at the acute corners, the strength of the worst singularity has been reduced. This is a considerable improvement since for the fractal any point on the boundary is arbitrarily close to both an obtuse and an acute corner. If the boundary consisted of only a few corners, for example the L-shaped domain, a different conformal map would be more suitable; see [26]. The improvement in smoothness may allow us to effectively use high order methods to compute the solution of the eigenvalue problem. The problem of solving the weighted eigenvalue problem is addressed in the next section.

5. Numerical solution of the transplanted eigenvalue problem

We first describe one way of discretizing the Laplacian on the unit disk. Here we follow closely the description given in Chapter 11 of [36]; see also [12]. The matrix arising from such a discretization is dense. The eigenfunctions of the transplanted problem are smooth inside the unit disk D, but not on its closure $\bar{D}$, as discussed in the previous section, and cannot be extended analytically outside the unit disk. This implies that the number of discretization points required for high accuracy will be quite large, which means that the discretization matrix will be both large and dense. For this reason we develop a method for fast inversion of such a matrix.

5.1. Spectral discretization of the Laplacian on a disk

We reformulate the problem by changing to polar coordinates

$$x = r \cos\theta, \quad y = r \sin\theta,$$

so that the weighted eigenvalue problem becomes

$$v_{rr} + r^{-1}v_r + r^{-2}v_{\theta\theta} + \lambda v|f'|^2 = 0, \quad \text{for } r < 1, \tag{10}$$
$$v = 0, \quad \text{for } r = 1.$$

Inspecting the above equations we can see that the point at the origin may prove to be a problem in the polar coordinate system. The governing equation is singular at $r = 0$ and whatever sensible range we restrict r and θ to, the origin will have an infinite number of representations in this system. This is an old and vexing problem that affects polar, spherical, cylindrical, and toroidal coordinates. A number of methods have been used to address this issue; for an extensive summary see [4]. The particular method we adopt is the one proposed by Fornberg [11,12] as realized in [36].

We discretize the disk by taking a periodic Fourier grid in θ and a non-periodic Chebyshev grid in r where

$$\theta \in [0, 2\pi], \quad r \in [-1, 1].$$

By a Fourier grid we mean M equally spaced points in the interval $[0, 2\pi]$ and the Chebyshev grid points are defined by $x_j = \cos(j\pi/N)$, $j = 0, 1, \ldots, N$. Even though this representation is not one-to-one it is often preferred to the more common one where

$$\theta \in [0, 2\pi], \quad r \in [0, 1].$$

The problem with the latter representation is that many of the discretization points are wastefully clustered near the origin. For the former representation the map (r, θ) to (x, y) is 2-to-1 and at the origin it is ∞-to-1. The problem at the origin can be avoided by choosing N to be odd. This trick appears effective in practice, though we do not know if there is a theoretical justification.

To be able to discretize equation (10) we need to construct discretized first and second derivatives on a Chebyshev grid and the second derivative on a Fourier grid. We give the definitions of the matrices involved but not direct formulas for their construction; these can be found in [36].

Let us define the discrete Fourier transform (DFT) of a vector $v \in \mathbb{R}^M$ to be the vector $\hat{v}$ with elements

$$\hat{v}_k = \frac{2\pi}{M} \sum_{j=1}^{M} \mathrm{e}^{-ikx_j} v_j, \quad k = -\frac{M}{2} + 1, \ldots, \frac{M}{2}, \tag{11}$$

where x_j are the Fourier grid points

$$x_j = 2\pi j/M, \quad j = 1, \ldots, M. \tag{12}$$

The inverse DFT is given by

$$v_j = \frac{1}{2\pi} \sum_{j=-M/2+1}^{M/2} \mathrm{e}^{ikx_j} \hat{v}_k, \quad j = 1, \ldots, M. \tag{13}$$

Given the vector of values of a function on the Fourier grid we can now compute the nth spectral derivative by the following procedure:

- Compute $\hat{v}$ from v.
- Define $\hat{w}_k = (ik)^n \hat{v}_k$. If n is odd, set $\hat{w}_{M/2} = 0$.
- Compute w from $\hat{w}$.

This operation is linear and hence the second derivative can be represented by a matrix $D_\theta^{(2)}$ or it can be performed by the use of the Fast Fourier Transform (FFT). In fact the above procedure is equivalent to first constructing the *trigonometric interpolant*

$$p(x) = \frac{1}{2\pi} \sum_{k=-M/2}^{M/2\,\prime} \mathrm{e}^{ikx} \hat{v}_k,$$

where the prime indicates that the terms $k = \pm M/2$ are multiplied by $\frac{1}{2}$, and then computing the nth derivative of the interpolant and evaluating it

$$w_k = p^{(n)}(x_k).$$

Similarly the spectral derivative of nth order w on a Chebyshev grid $(x_j)_{j=1}^N$, given function values $(v_j)_{j=1}^N$ on the same grid, is defined by the following two steps

- Let p be the unique polynomial of degree $\leqslant N$ such that $p(x_j) = v_j$.
- Define $w_j = p^{(n)}(x_j)$, where $p^{(n)}$ is the nth derivative of p.

This operation is again linear and hence can be represented by a matrix. It can also be performed by the use of the FFT, but we shall not make use of this fact. Let the first derivative be represented by a matrix D_r; then the second derivative is represented by the matrix D_r^2. We can impose homogeneous Dirichlet boundary conditions by requiring that the polynomial p from the above construction is zero at the boundary points ± 1. This requirement amounts to removing the first and last column and the first and last row of the differentiation matrices, giving new matrices $\widetilde{D}_r$ and $\widetilde{D}_r^2$ of size $(N-1)\times(N-1)$ for the first and second derivatives, respectively.

Now we are in a position to construct the discretized Laplacian for the unit disk. First we need to deal with the redundancy of our representation of points in the unit disk. Following [36], to understand how to deal with this redundancy let us consider solving the following $2K \times 2K$ system of linear equations where A_1, A_2, A_3, and A_4 are $K \times K$ matrices, and x_1, x_2, b_1, and b_2 are $K \times 1$ vectors

$$\begin{pmatrix} A_1 & A_2 \\ A_3 & A_4 \end{pmatrix} \begin{pmatrix} x_1 \\ x_2 \end{pmatrix} = \begin{pmatrix} b_1 \\ b_2 \end{pmatrix}.$$

If we know that $x_1 = x_2$ and that $b_1 = b_2$ then the system can be reduced to an $K \times K$ linear system: either $(A_1 + A_2)x_1 = b_1$ or $(A_3 + A_4)x_1 = b_1$. Accordingly we break up the differentiation matrices $\widetilde{D}_r$ and $\widetilde{D}_r^2$ into blocks as follows:

$$\widetilde{D}_r = \begin{pmatrix} E_1 & E_2 \\ E_3 & E_4 \end{pmatrix}, \quad \widetilde{D}_r^2 = \begin{pmatrix} D_1 & D_2 \\ D_3 & D_4 \end{pmatrix}.$$

Finally, the discretized Laplacian can be constructed from the above matrices by the use of Kronecker products

$$L = \begin{pmatrix} I & 0 \\ 0 & I \end{pmatrix} \otimes (D_1 + RE_1) + \begin{pmatrix} 0 & I \\ I & 0 \end{pmatrix} \otimes (D_2 + RE_2) + D_\theta^{(2)} \otimes R^2, \tag{14}$$

where I is the $M/2 \times M/2$ identity and R is a $(N-1)/2 \times (N-1)/2$ diagonal matrix which is the discrete equivalent of r^{-1} in Eq. (10). The last remaining term that needs to be discretized is the one corresponding to the derivative of the conformal map, $|f'|^2$ in (10). This is a diagonal matrix which we denote by F. With this the equation is discretized and to find discrete approximations to the eigenvalues and eigenfunctions of (10) we need to find the eigenvalues and eigenvectors of the matrix $F^{-1}L$. Note that since f is conformal inside the unit disk its derivative is never zero so the inverse of the diagonal matrix F is well-defined.

Now we can employ any suitable method for finding eigenvalues of a matrix to find approximations to the eigenvalues of the vibrating membrane. Since for reasonable accuracy the size of the matrix $F^{-1}L$ becomes very big we wish to solve the eigenvalue problem by an iterative solver. We apply Matlab's function `eigs`, which uses the Fortran package ARPACK [22,23], and requires a function that computes the product of the inverse of the matrix $F^{-1}L$ with an arbitrary vector. Since F is a diagonal matrix we concentrate on the inversion of L.

5.2. *Efficient inversion of the discretized Laplacian*

The cost of constructing the inverse of matrix L directly is $O(N^3M^3)$. To reduce the cost we turn to Fourier space. As we have seen from the derivation of the matrix $D_\theta^{(2)}$, the operator that it describes is diagonal in Fourier space; also the operator on the left-hand side of the second Kronecker product in (14) is diagonal in Fourier space since it is the convolution matrix of the vector $(0, 0, \ldots, 1, \ldots, 0)^T$, where 1 is in position M. So with variable θ transformed to

Fourier space the discretized Laplacian has the form

$$L_{\mathscr{F}} = I \otimes A_1 + Z \otimes A_2 + D \otimes A_3,$$

where

$$A_1 = D_1 + RE_1, \quad A_2 = D_2 + RE_2, \quad A_3 = R^2,$$

$Z = \mathrm{diag}((-1)^{i+1})$, $i = 1, \ldots, M$, and D is also an $M \times M$ diagonal matrix. It can be shown that the diagonal entries of D are the negative squares of integers; see [36].

The matrix $L_{\mathscr{F}}$ is block diagonal, hence the inverse is also block diagonal and can be computed by inverting the M diagonal blocks, $i = 1, \ldots, M$,

$$A_1 + (-1)^{i-1} A_2 + d_i A_3,$$

where A_1 and A_2 are $K \times K$ matrices as defined above, $K = (N-1)/2$, and d_i are diagonal elements of the matrix D. This is a simple case of the general formula $(A \otimes B)^{-1} = A^{-1} \otimes B^{-1}$, valid for any invertible A and B.

Note that A_3 is a diagonal matrix so it is cheap to find the inverse A_3^{-1}, hence it is sufficient to invert the following matrices

$$A_\pm + d_i I, \tag{15}$$

where $i = 1, \ldots, M$ and

$$A_\pm = A_3^{-1} A_1 \pm A_3^{-1} A_2. \tag{16}$$

The special structure of the subproblems can be used to solve the systems faster (see problem 7.4.3 in [14]). This can be done by using the real Schur decomposition to find orthogonal matrices $Q_\pm$ and upper triangular matrices $T_\pm$ such that

$$A_\pm = Q_\pm T_\pm Q_\pm^{\mathrm{T}}.$$

The cost of finding this decomposition is $\mathrm{O}(N^3)$. These matrices allow us to write

$$(A_\pm + d_i I)^{-1} = (Q_\pm T_\pm Q_\pm^{\mathrm{T}} + d_i Q_\pm Q_\pm^{\mathrm{T}})^{-1} = Q_\pm (T_\pm + d_i I)^{-1} Q_\pm^{\mathrm{T}}.$$

Hence it remains to invert M triangular matrices of size $K \times K$

$$T_\pm + d_i I,$$

the cost of which is $\mathrm{O}(MN^2)$.

To recapitulate, as a pre-calculation two Schur decompositions need to be performed, the cost of which is $\mathrm{O}(N^3)$, and inverses of M triangular matrices $T_\pm + d_i I$ need to be computed, the cost of which is $\mathrm{O}(MN^2)$. Once these matrices are computed the cost of matrix vector multiplication $L_{\mathscr{F}}^{-1} b$ is $\mathrm{O}(MN^2)$. The cost of moving to and fro Fourier space is of a lesser order $\mathrm{O}(MN \log MN)$.

5.3. Convergence of the spectral method

We do not give a rigorous error analysis. Instead, using the results on the regularity of the eigenfunctions, we attempt to justify our use of a spectral method for the transplanted eigenvalue problem. We do so by considering the one-dimensional approximation sub-problems in the r and in the θ directions. The following result will prove useful. The proofs can be found in [29,35].

Theorem 3. *Let $g(x)$ be a 2π-periodic function on $\mathbb{R}$ and let $g_M(x)$ be the trigonometric interpolant of degree $M/2$ in the equally spaced points $x_j = 2\pi j/M$, $j = 1, \ldots, M$. Then*

(*i*) *if g has a kth derivative in $[0, 2\pi]$ of bounded variation for some $k > v$ then* $\max_{x\in[0,2\pi]} |g^{(v)}(x) - g_M^{(v)}(x)| = \mathrm{O}(M^{-k+v})$ as $M \to \infty$.

(*ii*) *if g is analytic inside a strip of width 2η then* $\max_{x\in[0,2\pi]} |g^{(v)}(x) - g_M^{(v)}(x)| = \mathrm{O}(M^v \mathrm{e}^{-\eta M/2})$.

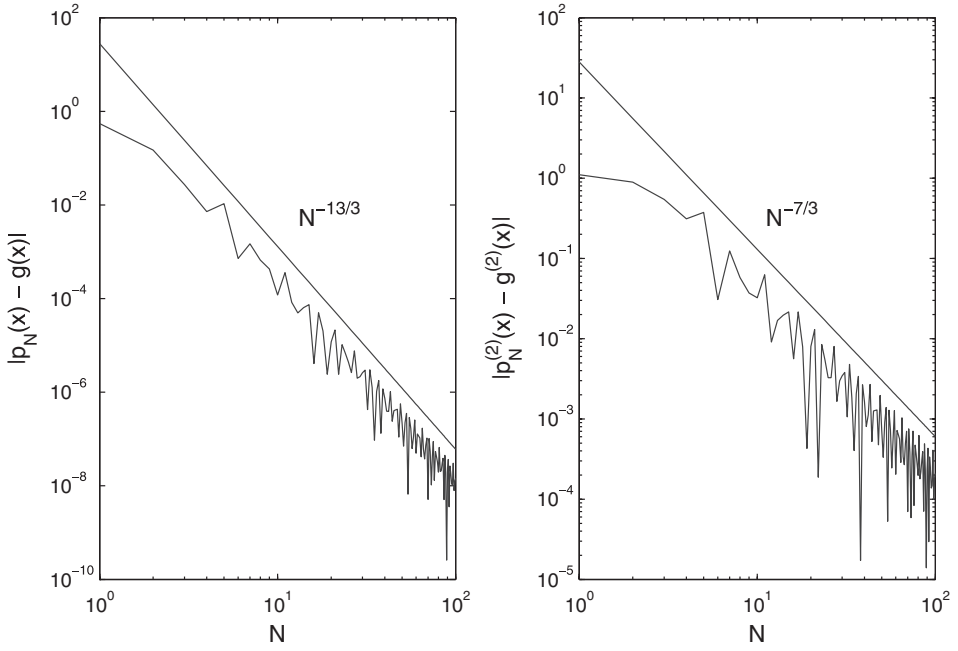

Fig. 3. The convergence of the polynomial interpolant in Chebyshev points of degree N, p_N, to the function $g(x) = (1 - x^2)^{5/3}$ is shown on the left. The convergence of the second spectral derivative is shown on the right. The errors are displayed at $x = 0.55$.

Let (λ, v) be a solution of the transplanted problem (4). For a fixed $r < 1$ the above result is applicable to the trigonometric interpolation in equally spaced points of the function $v_r(\theta) := v(r, \theta)$. Since v is C^∞ inside the unit disk, the discretization error decays faster than any fixed degree polynomial rate. This is true for any fixed $r < 1$, but for r close to one, the singularities are closer to the approximation interval which necessarily makes the errors larger. Theorem 3 can easily be extended to the case of continuous functions on the interval $[-1, 1]$, but to our problem this result is not be applicable since for any fixed θ, $v_\theta(r) := v(r, \theta)$ has a singularity on the boundary. In fact the second derivative of v_θ is unbounded on the interval $[-1, 1]$. The case of boundary singularities has been considered by Elliott [9]. For functions of the type $g(x) = (1 - x^2)^a g(x)$ where $g(x)$ is smooth everywhere on $[-1, 1]$, Elliott estimates the magnitude of the coefficients of the expansion of g in Chebyshev polynomials. In particular, if

$$g(x) = \sum_{n=0}^{\infty} a_n T_n(x),$$

where $T_n(\cdot)$ is the nth Chebyshev polynomial, it is shown that $a_n = \mathrm{O}(n^{-2a-1})$. Since the largest singularity of $v(r, \theta)$ is located on the boundary and has leading order $(1 - r)^{5/3}$ we consider the following model function:

$$g(x) = (1 - x^2)^{5/3}, \quad x \in [-1, 1].$$

Let p_N be the unique polynomial of degree $\leqslant N$ such that $p_N(x_j) = g(x_j)$, where $(x_j)_{j=1}^N$ is the Chebyshev grid. According to the result of Elliott we expect that $|p_N(x) - g(x)| = \mathrm{O}(N^{-13/3})$ for any fixed $x \in [-1, 1]$. Consequently, for the second spectral derivative approximation we expect that $|p_N^{(2)}(x) - g^{(2)}(x)| = \mathrm{O}(N^{-7/3})$, for any fixed $x \in (-1, 1)$. This is exactly what is observed in numerical experiments; see Fig. 3. By choosing Chebyshev points for collocation we ensure that the errors in the approximation of function g are roughly equally distributed along the interval $[-1, 1]$. However, since the second and higher derivatives of g are infinite at the boundary of the interval, we expect that the errors will be higher close to the boundary especially for the approximation of $g^{(2)}$. This is highlighted by Fig. 4. In fact increasing N does not improve the global error $\sup_{x\in(-1,1)} |p_N^{(2)}(x) - g^{(2)}(x)|$, but in contrast to Theorem 3 we

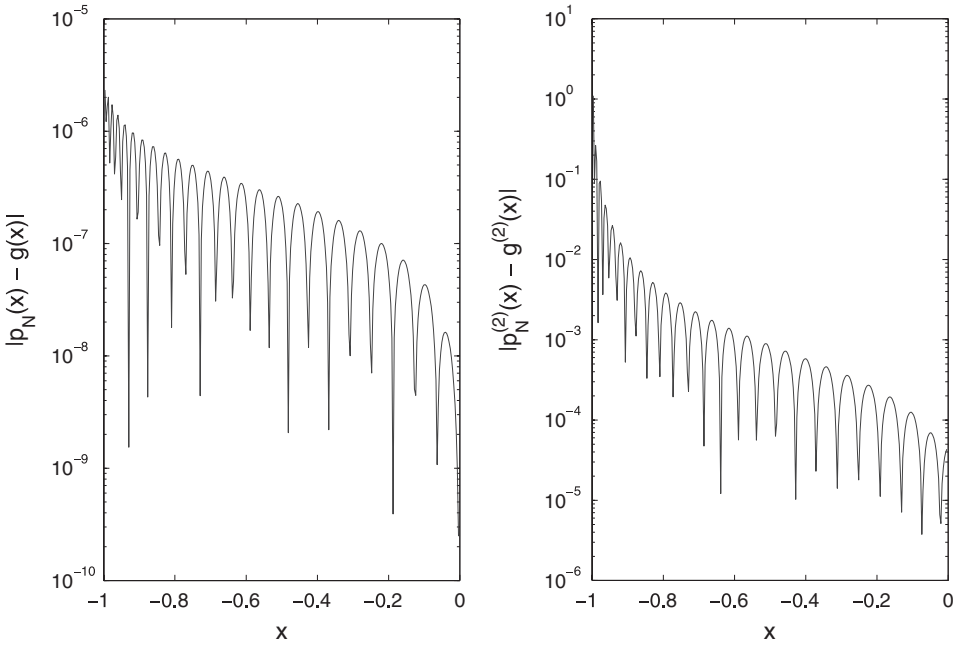

Fig. 4. Behaviour of the errors $|p_N(x) - g(x)|$ and $|p_N^{(2)}(x) - g^{(2)}(x)|$ for $N = 50$.

have that for any $\delta > 0$

$$\max_{x\in[-1+\delta,1-\delta]} |p_N^{(2)}(x) - g^{(2)}(x)| = \mathrm{O}(N^{-7/3}).$$

This suggests that our discretization of the function $v_\theta(r)$ may be inadequate. However, note that the value of v_θ at the boundary is known: $v_\theta(\pm 1) = 0$. Since $v_\theta(r)$ is at least once continuously differentiable on $[-1, 1]$ there will be a neighbourhood of ± 1 where the function will not change much from 0. If this neighbourhood is large enough, the errors we commit in the discretization of the second derivative near the boundary may not be crucial. We expect this neighbourhood to be smaller for higher eigenfunctions, consequently we expect that the accuracy will deteriorate for higher eigenvalues. We now proceed to the numerical results, which will support these informal statements.

6. Numerical results

In this section, we report on numerical results obtained by the methods described in the first half of the paper. For simplicity of implementation, for the most part, we do not use the symmetries of eigenfunctions but solve the eigenvalue problem on the whole domain. Nevertheless, numerical results suggest that this approach produces five or more digits of accuracy, depending on the eigenvalue, for the first 20 eigenvalues of the Koch snowflake fractal.

6.1. Choice of discretization points

Since the best available estimates found in the literature for the eigenvalues of the Koch snowflake or the polygons approximating it, which come from [20,27], are not accurate to more than three or four digits, we increase the number of points in the discretization of the unit disk and observe the change in eigenvalues of the discretized linear system. It is, however, not obvious how best to do this. There are two parameters: M, the number of discretization points in the θ direction, and $N + 1$, the number of points in the r direction. Recall that the total number of distinct discretization points is $M(N - 1)/2$.

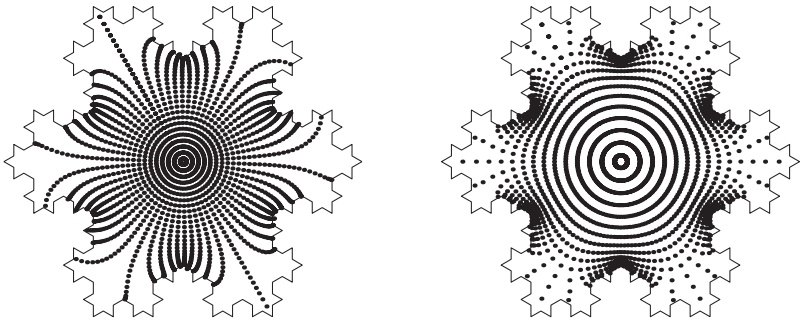

Fig. 5. Spectral collocation grid in the Koch snowflake keeping $M \approx N$ on the left and $M \approx 5N$ on the right. The number of points is approximately the same in the two plots, but the covering of the snowflake domain is much better in the second one.

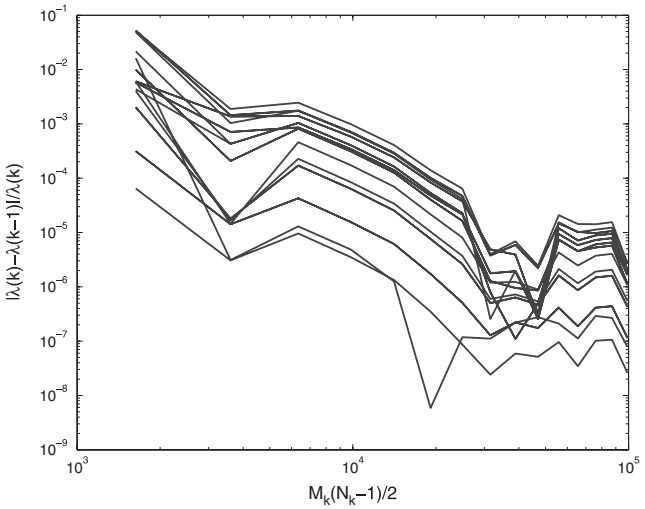

Fig. 6. Convergence of the first 20 eigenvalues of the polygon P_6 as the number of discretization points is increased. The discretization parameters are chosen so that $M_k \approx 12N_k$. Only 13 lines are visible due to the presence of repeated eigenvalues.

From extensive numerical investigation, as documented in [1], we concluded that for our purpose a good way of choosing the discretization parameters is to have the parameter M approximately 12 times larger than N. An indication as to why M should be chosen considerably larger than N can be obtained by looking at the image of the discretization points in the polygonal domain. In Fig. 5 it can be seen that with the same number of points the covering of the snowflake is much better if the parameter M is much larger than N. This is the consequence of a phenomenon of conformal mapping called *crowding*. Crowding also makes the computation of the conformal map f increasingly more difficult as the number of vertices is increased; due to this, particular care needs to be taken of numerical stability, for details see [1]. Because of the difference between the domains D and Ω groups of prevertices are crowded together, i.e., groups of singularities are crowded together which need to be resolved. Since we use evenly spaced discretization points in the θ direction we are forced to use a very large number of points in that direction.

The data obtained by choosing $M \approx 12N$ is displayed in Fig. 6; the precise numerical values can be found in [1]. From the convergence plot, we conclude that the eigenvalues of the particular polygon can be computed to around five or more digits for the first 20 eigenvalues. We now turn to the problem of approximating the eigenvalues on the Koch snowflake fractal. The hope is that these eigenvalues can also be computed to five or more digits.

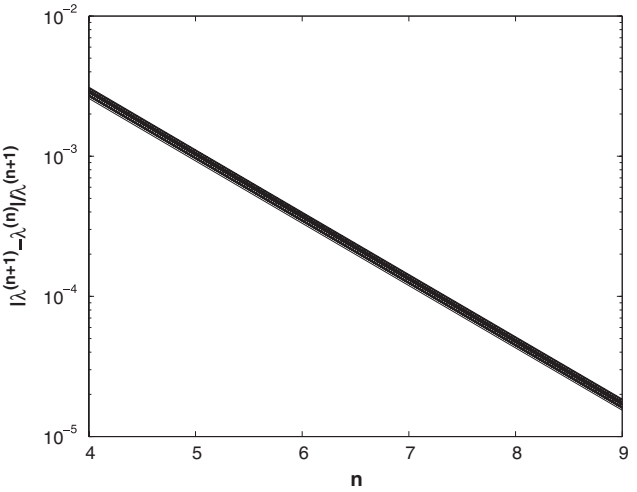

Fig. 7. Change in the first 20 eigenvalues of polygons P_n as the level is increased from $n = 4$ to $n = 10$.

6.2. *Change of eigenvalues with the change of fractal level*

Our ultimate goal is to compute the eigenvalues not on the polygonal domains but on the full fractal domain. We attempt to do this by solving the eigenvalue problem on a sequence of polygons P_n, $n \geqslant 1$, we defined recursively.

Let P_1 be the equilateral triangle with unit sides and P_{n+1} be the polygon obtained by replacing each side of the polygon P_n by the following generator element:


Hausdorff dimension $= \dfrac{\log 4}{\log 3}$.

As an example in Fig. 1 polygon P_3 is shown on the left and polygon P_4 on the right. Note that P_n is a polygonal approximation to the Koch snowflake with $3 \times 4^{n-1}$ vertices as defined. Note also that by construction P_{n+1} is a strict superset of P_n. The next step in the approximation of the eigenvalues of the fractal is to compute the eigenvalues of increasingly better polygonal approximations to the fractal.

We perform computations for polygons P_4 up to P_{10}, with the discretization parameters related as $M \approx 12N$, and observe almost identical convergence curves as shown in Fig. 6 for P_6. Hence we decide to use the same choice of discretization parameters for each polygon. We choose $M = 1530$ and $N = 125$. These numbers are somewhat larger than the ones used to obtain the final data point in Fig. 6. The computation of the conformal map is done by the C++ code developed using the methods described in [2] and the solution of the eigenvalue problem is done using Matlab. For the above choice of discretization parameters, the time needed to invert the discretized laplacian, which is an $O(N^3) + O(MN^2)$ process, is around 280 s on a Pentium III 800 MHz processor. If the position of the prevertices is already known and all the expansions in the fast multipole algorithm have already been computed, the computation of the derivative of the SC map at the discretization points takes around 27 s irrespective of the number of vertices of the polygon. Once the linear systems are inverted and the SC integrand is computed, a further 455 s are needed to solve the resulting eigenvalue problem for the first 20 eigenvalues.

To see how well the eigenvalues of the Koch snowflake are approximated by the eigenvalues of these polygons we plot the relative change in eigenvalues as the level of approximation to the snowflake is increased; see Fig. 7. The plot suggests that 10th level of approximation to the fractal is enough to obtain about five digits of accuracy for the eigenvalues. The convergence seems very close to linear and we may try and use this regularity to accelerate the convergence.

A suitable extrapolation method in this case is Aitken's Δ^2 method; see for example [16,34]. Next we plot the convergence curves of the accelerated sequence; see Fig. 8. We see that some of the lines still look very straight and hence may allow for a further application of Aitken's Δ^2 method. The improvement obtained by a single application of the extrapolation method is sufficient to allow for around eight digits of the eigenvalues of the fractal. However, we

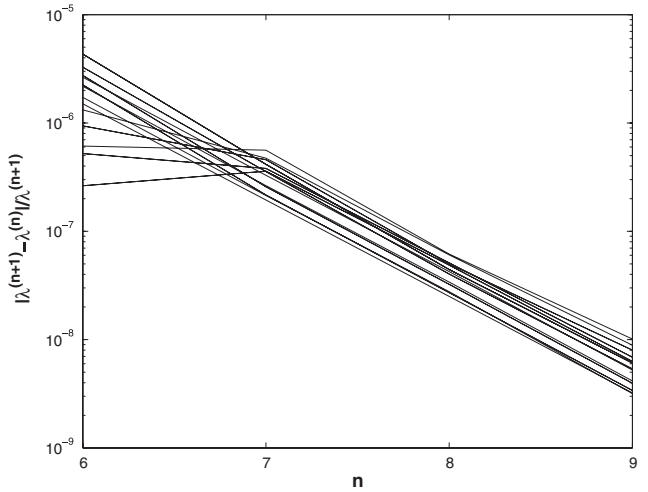

Fig. 8. Accelerated convergence to the eigenvalues of the Koch snowflake.

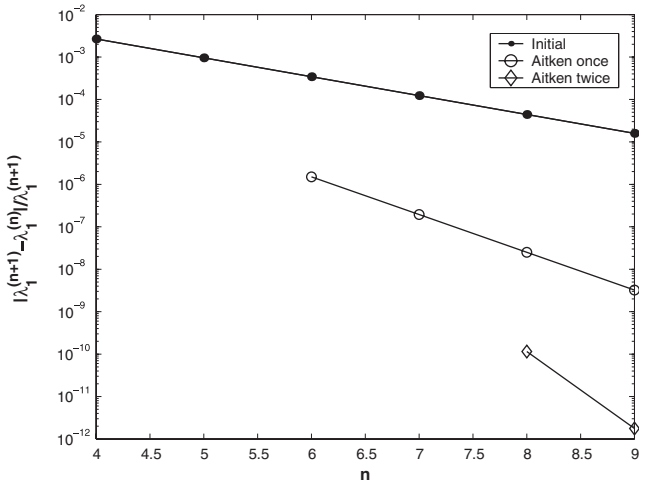

Fig. 9. Acceleration of the convergence to the first eigenvalue of the Koch snowflake as Aitken's Δ^2 method is applied twice.

can only obtain the full eight digits if the initial computation of the eigenvalues on the polygons were equally accurate. The only eigenvalue, on the polygons, that we computed to about eight digits is the first eigenvalue. For this case we applied Aitken's method twice and obtained the convergence curves shown in Fig. 9.

Hence, it turns out that by accelerating convergence we obtain as many digits for the eigenvalues of the Koch snowflake as the accuracy of the eigenvalues on the polygons allows us to have; see Table 1 for the results in the case of the first eigenvalue. In Table 2 we give our best guess for the first 20 eigenvalues. See Fig. 10 for contour plots of some eigenfunctions on the unit disk and Fig. 11 for the same eigenfunctions mapped onto the snowflake domain.

6.3. Making use of symmetries

We know that both the snowflake fractal and the approximating polygons have six lines of symmetry; if the snowflake is oriented as in Fig. 1 and centred at the origin the lines of symmetry are radial lines at angles that are integer multiples of $\pi/6$. In particular, the real and the imaginary axes are two lines of symmetry. Let u be an eigenfunction with eigenvalue λ of the eigenvalue problem (3). Then it is easy to check that $u(x, -y)$ is also an eigenfunction with eigenvalue λ and

Table 1
Accelerating the convergence to the first eigenvalue on the fractal by Aitken's Δ^2 method

n	$\lambda_1^{(n)}$	$\hat{\lambda}_1^{(n)}$	$\hat{\hat{\lambda}}_1^{(n)}$
4	39.51229200544		
5	39.40725888240		
6	39.36962897131	39.34862091891	
7	39.35612308145	39.34856177733	
8	39.35127249174	39.34855413187	39.34855299677
9	39.34953001618	39.34855314694	39.34855300129
10	39.34890401525	39.34855302011	39.34855300136

Table 2
Eigenvalues of the Koch snowflake, correct to the number of digits shown with doubt over the last digit

k	λ_k	k	λ_k
1	39.348553	11	314.44
2	97.43691	12	314.44
3	97.43691	13	359.51
4	165.406	14	425.38
5	165.406	15	443.52
6	190.370	16	443.52
7	208.608	17	458.65
8	272.406	18	458.65
9	272.406	19	560.38
10	312.3538	20	560.38

hence so are

$$u(x, y) \pm u(x, -y)$$

if nonzero. The same holds for

$$u(x, y) \pm u(-x, y).$$

So for any eigenvalue we can assume that its eigenfunction is either symmetric (even) or antisymmetric (odd) about the real and imaginary axes. The use of symmetries to simplify the computation of eigenvalues is well known; for example, it was famously used to compute the eigenvalues of the L-shaped domain in [13].

If the conformal map of the unit disk D to the Koch snowflake Ω is such that it preserves the symmetries, i.e. if the prevertices are symmetric with respect to the same six lines, then in the same way as for Ω the eigenfunctions of the weighted eigenvalue problem on the unit disk split into symmetry classes. If we concentrate on finding eigenfunctions with particular symmetries our discretization becomes wasteful.

There is a simple way of exploiting the symmetries of eigenfunctions. For example, the eigenfunctions that are antisymmetric with respect to the real and imaginary axes are zero on these axes, so it is enough to solve the same eigenvalue problem on just a quarter of the snowflake. The redundancy of the discretization can be dealt with in the same way as in Section 5.1. Another possibility is to transplant the problem on a slice of the fractal polygon to the unit disk. This can be done by first mapping the unit disk to the quarter of the unit disk in the first quadrant and then mapping this slice to the slice of the Koch snowflake polygon with the same symmetric Schwarz–Christoffel map as before. With this the size of the discretized Laplacian has been significantly reduced for the same density of discretization points and the methods developed in the previous sections are all applicable. Also the freedom in the choice of the map from the disk to the quarter disk can be used to improve the convergence. For symmetry classes in which eigenfunctions have at least one line of even symmetry the situation is a bit more complicated since we need to be able to impose homogeneous Neumann as well as Dirichlet boundary conditions.

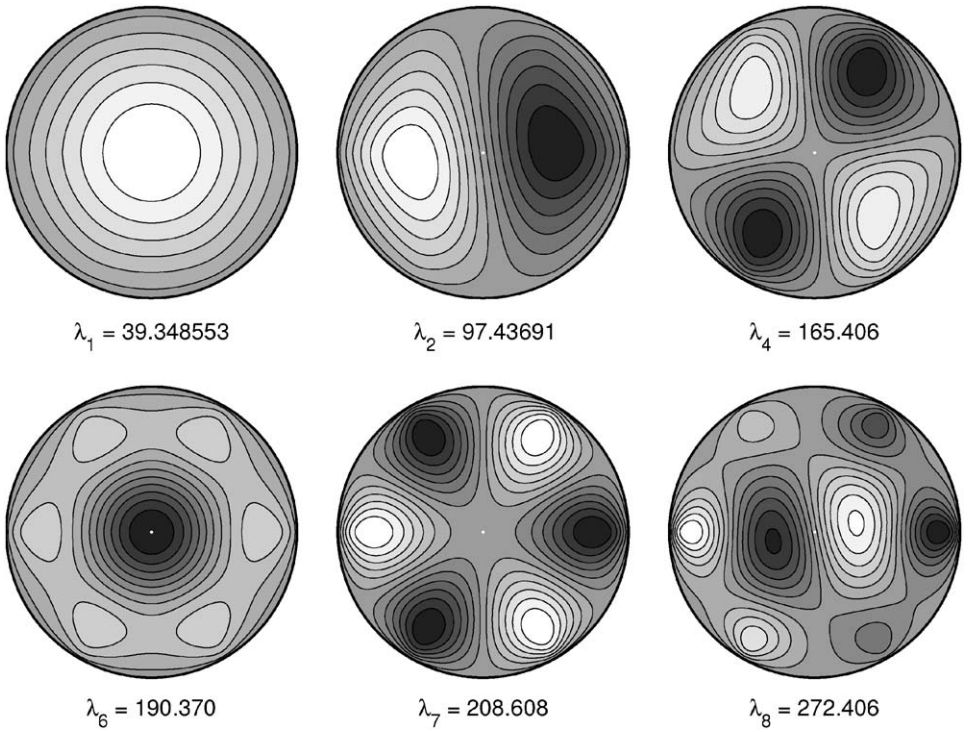

Fig. 10. The first, second, fourth, sixth, seventh, and eight eigenfunctions of the transplanted eigenvalue problem on the unit disk.

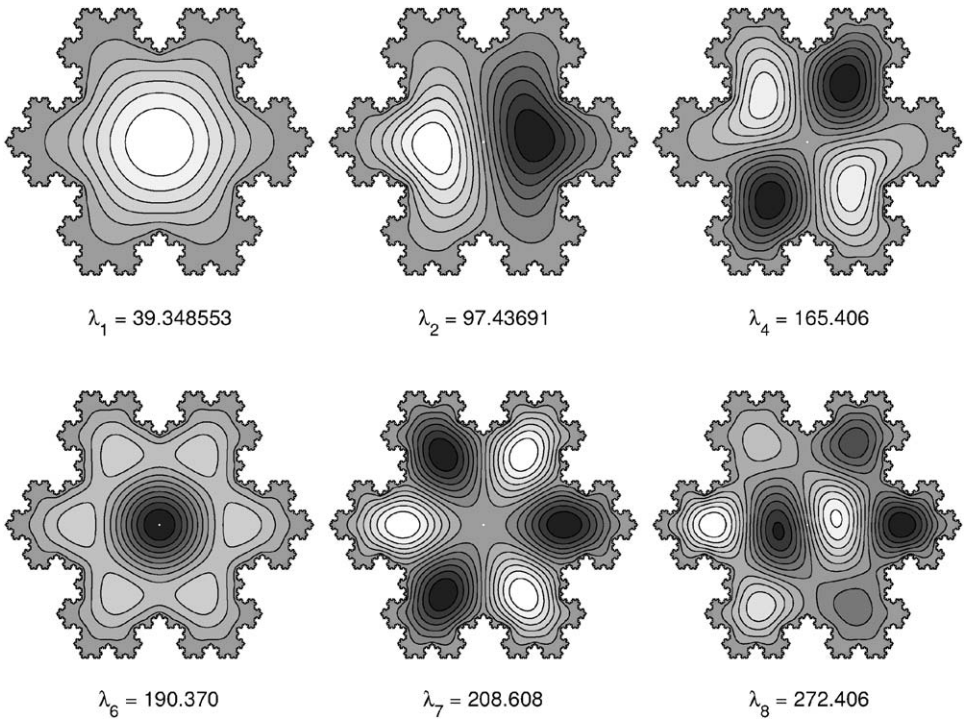

Fig. 11. The first, second, fourth, sixth, seventh, and eight eigenfunctions on the Koch snowflake.

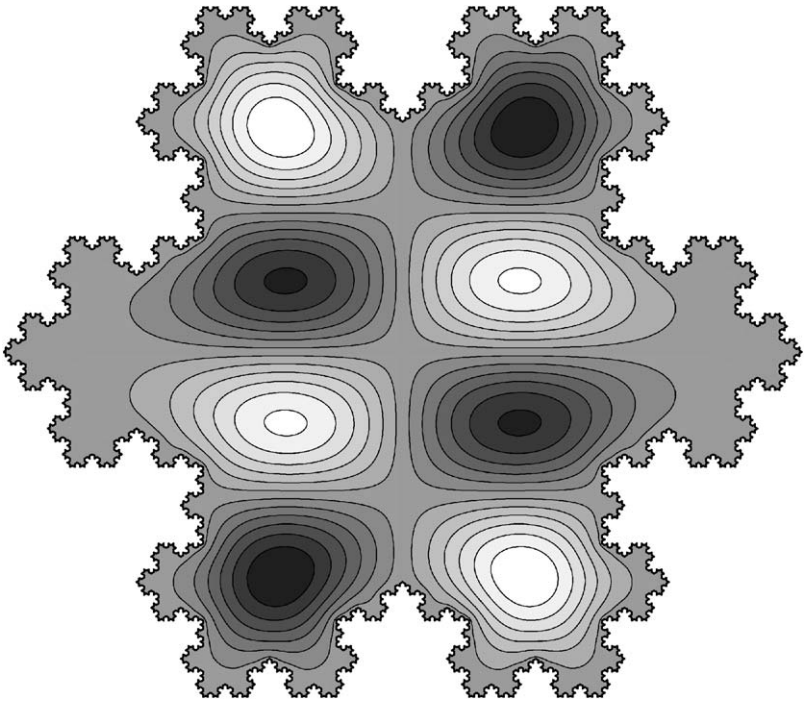

Fig. 12. Eleventh eigenfunction, antisymmetric with respect to the real and imaginary axes.

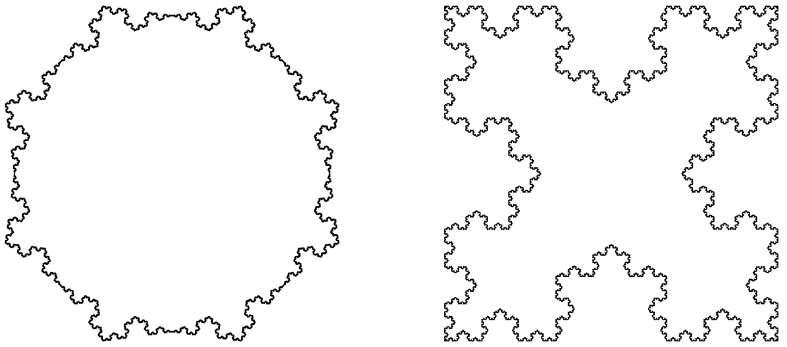

Fig. 13. For the fractal on the left we have been able to obtain six digits for the first 20 eigenvalues whereas for the fractal on the right only 3.

Looking at Table 2 it can be seen that the overall trend is slower convergence for the higher eigenvalues. However, more accurate estimates can be obtained if symmetries are used. To illustrate this we computed the first 2 eigenfunctions that are antisymmetric with respect to the real and imaginary axes. The same ratio for the discretization parameters as before proved to be appropriate and Aitken's method was used again to obtain an estimate of the eigenvalues on the fractal. Using this approach, we obtain more digits for the 4th and 5th, and 11th and 12th, eigenvalues, namely $\lambda_4 = \lambda_5 = 165.4058$ and $\lambda_{11} = \lambda_{12} = 314.444$. A contour plot of the 11th eigenfunction is shown in Fig. 12.

6.4. More fractals

We have also computed the eigenvalues for two other fractals. For the fractal on the left in Fig. 13 we have obtained six digits for all of the first 20 eigenvalues whereas for the one on the right only 3 for higher eigenfunctions; see Fig. 14. The lack of accuracy obtained for the second fractal is due to the extreme crowding caused by the elongations

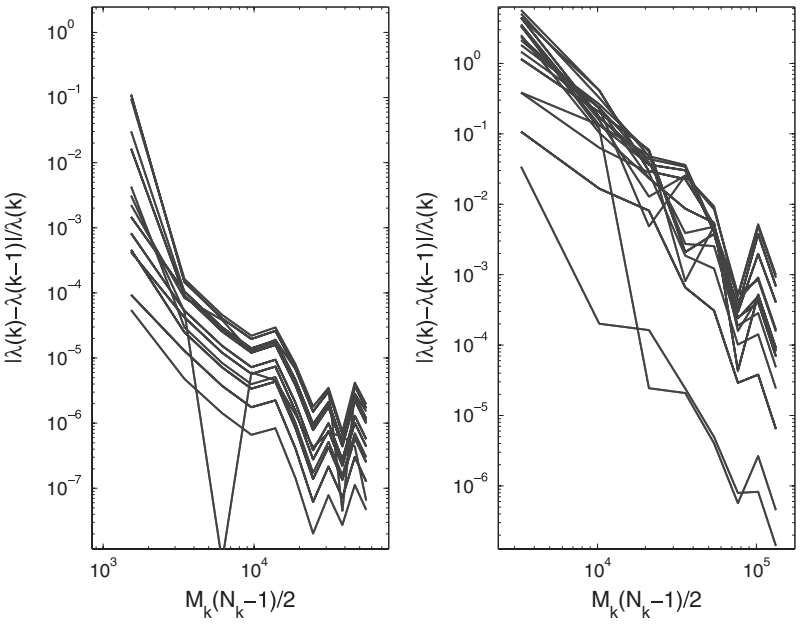

Fig. 14. Convergence curves of eigenvalues for the fractals shown in Fig. 13. Note the different horizontal scales.

in the fractal domain. To compensate for the crowding we had to choose many more points in the angular direction than for the Koch snowflake. We chose $M \approx 60N$ to obtain the convergence plot on the right of Fig. 11).

7. Conclusion

To solve the eigenvalue problem on the Koch snowflake, we have approximated the fractal with a polygon with many sides, mapped the polygon to the unit disk with a Schwarz–Christoffel map implemented with the aid of multipole expansions, and solved a new eigenvalue problem. The new problem has a much simpler computational domain and also the eigenfunctions are smoother allowing for an effective use of a spectral collocation method. The convergence to the eigenvalues of the fractal is slow with the increase of the level of polygonal approximation to the fractal, however, we were able to accelerate this convergence by the use of Aitken's Δ^2 method. Consequently, it turns out that what limits our accuracy for higher eigenfunctions is not the poor approximation of the fractal boundary but the accuracy of the numerical solution of the eigenvalue problem on the unit disk. One of the reasons for this is the restriction on the collocation points in our algorithm. It would be interesting to try other methods than spectral collocation to solve the eigenvalue problem on the disk. Methods that allow more freedom in the choice of discretization could especially be favourable for fractals with elongations. These would include an *hp*-finite element method [33] and perhaps most in the spirit of the paper, a radial basis functions method [28]. Transplantation to domains with similar elongations to counter the phenomenon of crowding could also be considered; see [17].

Acknowledgements

I am grateful to Nick Trefethen for many valuable suggestions throughout the course of this work and to André Weideman for interesting discussions and for pointing me to the relevant literature.

References

[1] L. Banjai, Computation of Conformal Maps by Fast Multipole Method Accelerated Schwarz–Christoffel Transformation, Ph.D. Thesis, Oxford University, England, 2003.
[2] L. Banjai, L.N. Trefethen, A multipole method for Schwarz–Christoffel mapping of polygons with thousands of sides, SIAM J. Sci. Comput. 25 (3) (2003) 1042–1065.
[3] T. Betcke, L.N. Trefethen, Reviving the method of particular solutions. SIAM Rev. 47 (2005) 469–491.
[4] J.P. Boyd, Chebyshev and Fourier Spectral Methods, second edition, Dover Publications Inc., Mineola, NY, 2001.
[5] L.M. Cureton, J.R. Kuttler, Eigenvalues of the Laplacian on regular polygons and polygons resulting from their dissection, J. Sound Vibration 220 (1) (1999) 83–98.
[6] E.B. Davies, Spectral Theory and Differential Operators, Cambridge Studies in Advanced Mathematics, vol. 42, Cambridge University Press, Cambridge, 1995.
[7] T.A. Driscoll, Eigenmodes of isospectral drums, SIAM Rev. 39 (1) (1997) 1–17.
[8] T.A. Driscoll, L.N. Trefethen, Schwarz–Christoffel Mapping, Cambridge University Press, Cambridge, 2002.
[9] D. Elliott, The evaluation and estimation of the coefficients in the Chebyshev series expansion of a function, Math. Comput. 18 (1964) 274–284.
[10] C. Ferguson, Helaman Ferguson, Meridian Creative Group, Erie, PA, 1994.
[11] B. Fornberg, A pseudospectral approach for polar and spherical geometries, SIAM J. Sci. Comput. 16 (5) (1995) 1071–1081.
[12] B. Fornberg, A Practical Guide to Pseudospectral Methods, Cambridge University Press, Cambridge, 1996.
[13] L. Fox, P. Henrici, C. Moler, Approximations and bounds for eigenvalues of elliptic operators, SIAM J. Numer. Anal. 4 (1967) 89–102.
[14] G.H. Golub, C.F. Van Loan, Matrix Computations, third edition, Johns Hopkins University Press, Baltimore, MD, 1996.
[15] C.A. Griffith, M.L. Lapidus, Computer graphics and the eigenfunctions for the Koch snowflake drum, in: Progress in Inverse Spectral Geometry, Trends Math., Birkhäuser, Basel, 1997, pp. 95–113.
[16] P. Henrici, Elements of Numerical Analysis, Wiley, New York, 1964.
[17] L.H. Howell, Computation of Conformal Maps by Modified Schwarz–Christoffel Transformations. Ph.D. Thesis, Massachusetts Institute of Technology, 1990.
[18] J.R. Kuttler, V.G. Sigillito, Eigenvalues of the Laplacian in two dimensions, SIAM Rev. 26 (2) (1984) 163–193.
[19] M.L. Lapidus, Fractals and vibrations: can you hear the shape of a fractal drum?, Fractals 3 (4) (1995) 725–736 (Symposium in Honor of Benoit Mandelbrot (Curaçao, 1995)).
[20] M.L. Lapidus, J.W. Neuberger, R.J. Renka, C.A. Griffith, Snowflake harmonics and computer graphics: numerical computation of spectra on fractal drums, Internat. J. Bifurc. Chaos Appl. Sci. Eng. 6 (7) (1996) 1185–1210.
[21] M.L. Lapidus, M.M.H. Pang, Eigenfunctions of the Koch snowflake domain, Comm. Math. Phys. 172 (2) (1995) 359–376.
[22] R.B. Lehoucq, D.C. Sorensen, Deflation techniques for an implicitly restarted Arnoldi iteration, SIAM J. Matrix Anal. Appl. 17 (4) (1996) 789–821.
[23] R.B. Lehoucq, D.C. Sorensen, C. Yang, ARPACK Users' Guide, SIAM, Philadelphia, PA, 1998.
[24] B.B. Mandelbrot, Fractals: Form Chance and Dimension, revised edition, W.H. Freeman and Co., San Francisco, 1977.
[25] B.B. Mandelbrot, The Fractal Geometry of Nature, W.H. Freeman and Co., San Francisco, 1982.
[26] J.C. Mason, Chebyshev polynomial approximations for the *L*-membrane eigenvalue problem, SIAM J. Appl. Math. 15 (1967) 172–186.
[27] J.M. Neuberger, N. Sieben, J.W. Swift, Computing eigenfunctions on the Koch Snowflake: A new grid and symmetry, J. Comput. Appl. Math., 2005, to appear.
[28] R.B. Platte, T.A. Driscoll, Computing eigenmodes of elliptic operators using radial basis functions, Comput. Math. Appl. 48 (3–4) (2004) 561–576.
[29] S.C. Reddy, J.A.C. Weideman, The accuracy of the Chebyshev differencing method for analytic functions, SIAM J. Numer. Anal., to appear.
[30] B. Sapoval, Fractals, Aditech, Paris, 1990.
[31] B. Sapoval, T. Gobron, A. Margolina, Vibrations of fractal drums, Phys. Rev. Lett. 67 (21) (1991) 2974–2978.
[32] R. Schinzinger, P.A.A. Laura, Conformal Mapping: Methods and Applications, Elsevier Science Publishers B.V., Amsterdam, 1991.
[33] C. Schwab, *p*- and *hp*-Finite Element Methods, The Clarendon Press, Oxford University Press, New York, 1998.
[34] A. Sidi, Practical Extrapolation Methods, Cambridge University Press, Cambridge, 2003.
[35] E. Tadmor, The exponential accuracy of Fourier and Chebyshev differencing methods, SIAM J. Numer. Anal. 23 (1) (1986) 1–10.
[36] L.N. Trefethen, Spectral Methods in MATLAB, SIAM, Philadelphia, PA, 2000.
[37] T.A. Witten, L.M. Sander, Diffusion-limited aggregation a kinetic critical phenomenon, Phys. Rev. Lett. 47 (1981) 1400–1403.